The effectiveness of a snow fence in the dry Andes region of Chile

C.D.Q. Antonissen

26/01/2018

TU Delft

The effectiveness of a snow fence in the dry Andes region of Chile

by

C.D.Q. Antonissen

Student number: 4219376
Project duration: September 11, 2017 – December 1, 2017
Thesis committee:
Dr. S.L.M Lhermitte, TU Delft
Dra. S. MacDonell, CEAZA
Dra. N. Schaffer, CEAZA
Dr. R.C. Lindenbergh, TU Delft

TU Delft

Preface

This report was written in order to finish the project on snow fences in the Andes mountains in Region IV in Chile. It was undertaken at CEAZA in La Serena, Chile. Doing research and writing this report while being abroad has been an enlightening, useful and above all an amazing experience. The combination of an excellent working environment in the office and three wonderful fieldworks in the gorgeous surroundings of snow fences made it an unforgettable experience.

First of all I would like to thank Nicole Schaffer, who helped me a lot by providing ideas and suggestions for the project. It was great to always be able to ask questions and have discussions. She also provided a lot of help for writing this report.

I would also like to thank Stef Lhermitte and Shelley MacDonell who both had helpful suggestions and remarks on my work. And above all, whom without I would not have been here in Chile.

Also lots of thanks to Marion Reveillet and Roderick Lindenbergh. Marion helped me out mostly with questions regarding modelling of snow and Roderick gave useful and eye-opening remarks on my first draft version of this report.

Last but not least, I would like to thank the guys I have been sharing my office with in the past months: Robin, Eduardo, Marcello, Andrès and Dirk, you guys are great and it was a lot of fun working with you!

Coco Antonissen
La Serena, January 2018

Contents

List of Figures

List of Tables

1 Introduction

Water is an important, if not the most important, source that serves the needs of humans. But, not everywhere on Earth water is present in abundance. One of those places is the region Coquimbo, the 4^{th} region of Chile (Salinas et al, 2016; Verbist et al, 2008). This region is one of the regions located adjacent to the dry Andes, which stretches from the Atacama desert in the north of Chile to 35°S in Chile, and is the most arid part of the cordillera (Lliboutry, 1998). The average precipitation in this region at elevations lower than 750 m asl is ~120 mm/year, of which almost all precipitation occurs in the months of May to September (Favier et al, 2009). With very little precipitation during spring and summer, water supply in these seasons depends mostly on melt water from snow in the Andes mountains (Favier et al, 2009).

Furthermore, long lasting dry periods are not uncommon and may bring periods of 12 consecutive months without precipitation. ENSO (El Niño Southern Oscillation) has a major impact on the interannual variability of precipitation. Usually during the warm phase of ENSO, precipitation is higher than usual (Aceituna, 1998; Rutllant and Fuenzalido, 1991; Escobar and Aceituno, 1998; Ginot et al, 2006).

Since water supply in the region during summer is scarce and highly dependent on the melt of snow from the Andes mountains it is important that snow melts and does not sublimate. Furthermore, it is desirable to have a stream flow from melting snow for a long period after winter. However, the snow cover generally lasts for only 1 to 2 months after the last winter snowfall (Favier et al, 2009).

Because of a decreasing trend of precipitation in the last century (Le Quesne et al, 2006), and the growing demand for water in the region, a discrepancy between supply and demand exists. Working towards finding possible solutions, an effort is made to evaluate the effect of snow fences in the Andes mountains.

Previous research on snow fences, both in the simulation environment as well as by using field observations, has proved the effectiveness of snow fences (Alhajraf, 2003; Iversen, 1981; Tabler, 1980; Bang et al, 1994). Placing snow fences is a relatively low-cost possibility. The operation of a snow fence is based on wind reduction at the leeward side of the fence (Tabler, 1991). A detailed explanation of the operation of a snow fence is given in section 2.2.

No research was found on the effect of a snow fence on the ratio between sublimation and melt of snow. However, snow fences are known to reduce wind speed. This results in a change in the ratio between sublimation and melt in favor of melt (Fujita et al, 2010; Mott et al, 2013; Dadic et al, 2013). Another reason for the relative decrease in sublimation is that the snow stays in place for a longer period during which the temperature rises. This is discussed more extensively in section 2.1.

A change in the ratio between sublimation and melt can potentially make a very large difference in the region because sublimation can account for extremely high losses of the total accumulation (Ginot et al, 2006). On average, sublimation accounted for 46% of the total ablation at the Tapado glacier between 1962-1999, a glacier located close to Llano de las Liebres (Ginot et al, 2006). With a peak in 1981 when sublimation was responsible for 84% of the ablation, it is clear that by relatively lowering sublimation a big impact on the amount of water run-off can be made.

Because research sites in the Andes mountains are remote and, especially during winter with snow, hard or impossible to reach, projects must be monitored remotely. To monitor snow cover over large areas, satellite imagery is widely used. However, it is impossible to determine snow depth using satellite imagery. Also, satellite images are not very useful to monitor the variability of snow cover and snow depth on a smaller scale. Another problem often encountered using satellite imagery is its temporal resolution. For the monitoring

of daily snow depth changes, satellite imagery can therefore not be used. Instead, digital camera images combined with snow stakes have proved to be very effective (Dong and Menzel, 2017; Hinkler et al, 2002; Parajka et al, 2012). Using this method, snow depth can be determined in both spatial and temporal high resolution.

The research project presented in this report is conducted by CEAZA (**C**entro de **E**studios **A**vanzados en **Z**onas **Á**ridas), which is a research institute based in the cities of La Serena and Coquimbo. The glaciology group of CEAZA is funded by the regional government of Coquimbo to evaluate the effectiveness of snow fences in the Andes mountains. Because of the increased demand for water in the region, snow fences may be installed on a larger scale if they prove to be a useful technology.

1.1. Objectives

The quantitative effect of snow fences in the Andes mountains under different circumstances is unknown. Furthermore, the best way to analyze the snow depth using the daily digital camera images must be investigated. Therefore, the aim of this project is twofold. The first goal is to get a qualitative as well as a quantitative idea of the effect of a snow fence in the Andes mountains in Region IV in Chile. In particular, the following questions associated to the first goal of this project will be answered:

1. **Do snow fences in Region IV enhance the accumulation of snow and prolong the amount of time snow stays on the ground?**

2. **How much additional snow is accumulated due to the presence of the snow fences?**

To answer these questions, daily camera images of the snow fence and associated network of stakes were used to evaluate the pattern of snow depth distribution over time. The total volume of snow bounded by the stake network and additional fraction of snow present due to the presence of a snow fence were calculated. The site setup and methodology are discussed in chapter 3.

From the photos that are obtained, snow depths can be derived in different ways. Therefore, the second aim of this project will be answered by the third research question:

3. **What is the most optimal method to determine snow depths around a snow fence using snow stakes and digital camera images?**

2 Theory

2.1. Ablation, sublimation and melt

To better understand the importance and reasoning for testing the effectiveness of snow fences, one must be familiar with the concepts *ablation*, *sublimation* and *melt*.

In terms of snow, ablation is the combined result of processes such as sublimation and melt that remove snow from a snow surface[1].

If ablation takes place via melt, solid snow converses to liquid: water runs off the snow pack. With sublimation the snow directly converses from the solid phase to the gaseous phase, without becoming water first[2]. This means that a part of the potential water source is wasted into the atmosphere.

The ratio between melt and sublimation varies. It is likely that for thicker snow packs, sublimation is relatively less because relatively less snow is in contact with air. But above that, a thicker snow pack means that the snow will stay in place longer in the season. Because in winter time, with temperatures below 0°C, no melt occurs, all ablation takes place via sublimation. Later in the season more ablation via melt will take place due to higher temperatures.

Furthermore, sublimation is higher in areas with low air humidity, high solar radiation and strong winds (Gascoin et al, 2013). Especially wind has a big impact on sublimation and with that also on the ratio between sublimation and melt of snow (Fujita et al, 2010; Mott et al, 2013; Dadic et al, 2013).

2.2. The snow fence and its principle

In the technical report written by R.D. Tabler of Tabler & Associates in 1991, the principle of a snow fence is explained. The idea of a snow fence is that it reduces wind speed, allowing the creeping and saltating (intermittently jumping) particles to come to rest (Tabler, 1991).

Since the fence is placed such that it is orientated perpendicular to the main wind direction it is possible to speak about upwind and downwind sides of the fence. The fence causes the wind to slow down ahead of the snow fence. Therefore, some snow deposits upwind of the fence. However, most of the snow will accumulate downwind of the snow fence. The effect of a snow fence can be split up into four stages (Tabler, 1991):

1. Initially a lens-shaped drift is formed because creeping and saltating particles are caught by the fence. This is marked in Figure 2.1 by profile number 1. The spatial extent of the decrease in wind force depends on the height of the fence: the fence has in this stage an effect up until about 15 times the height of the fence.

2. During stage two this lens-shaped deposit grows and becomes deeper until the wind no longer follows its curvature. An eddy or recirculation zone at the downwind side of the lens occurs, causing particles to be trapped: a slip face is formed (profiles 2 and 3 in the Figure).

3. The third stage starts when the snow accumulation has reached its maximum depth, which is about 1 to 1.2 times the height of the fence for a 50% porous fence. This stage is marked in Figure 2.1 with profiles

[1] https://nsidc.org/cryosphere/glossary/term/ablation
[2] https://nsidc.org/cryosphere/glossary/term/sublimation

4-6. Because the recirculation zone shrinks, trapping efficiency decreases. However, the amount of accumulated snow keeps increasing. The extent of the effect of snow fence now reaches a distance of 20 times the height of the fence.

4. In the last stage (profile 7 in Figure 2.1) the recirculation zone disappears and the snow accumulation forms a smooth profile without a slip face. Compared to the ends of the fence, more snow accumulates in the middle part (Bang et al, 1994).

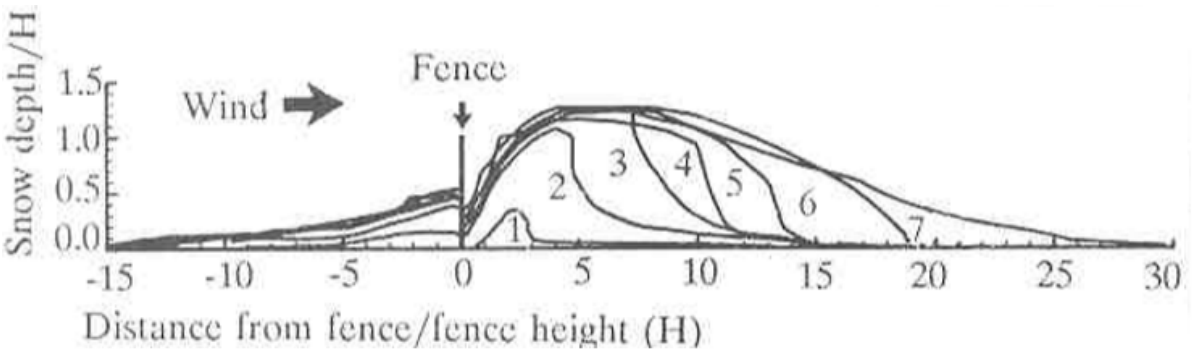

Figure 2.1: A sketch of the different stages of the effect of a snow fence with 50% porosity. This image is taken from the technical report of R.D. Tabler [18].

3

Methodology

The study sites, snow fence dimensions and grid of snow stakes are discussed in, respectively, sections 3.1, 3.2 and 3.3. Section 3.4 discusses the data collection and section 3.5 discusses the different methods for snow depth calculation. Sections 3.6 and 3.7 elaborate on the visualization of the results and volume calculations.

3.1. Study sites

Snow fences were placed in two different study sites that are called Tascadero and Llano de las Liebres. The latter will be abbreviated to Llano for the rest of the report. Both sites are located in the Andes in region IV of Chile (Figure 3.1).

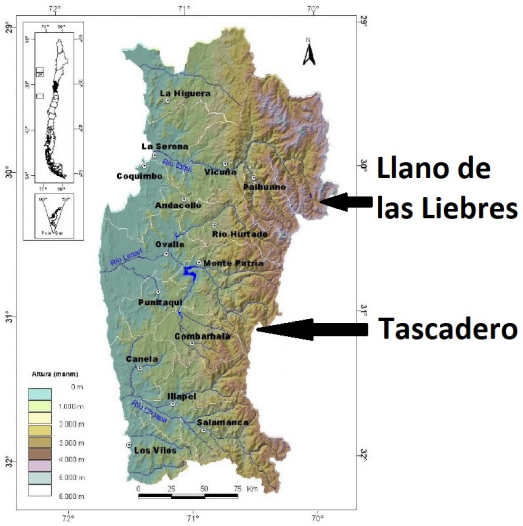

Figure 3.1: A sketch of the test locations Tascadero and Llano[1]. The arrow marked with number one indicates the location of Tascadero. The arrow marked with number two indicates the location of Llano.

In Table 3.1, relevant characteristics of Tascadero and Llano are listed. Temperature, wind, solar radiation and humidity are measured by weather stations installed at the test sites. The most significant differences are found in surface inclination (25° and 0°) and aspect (135° and 0°). Furthermore, a difference in surrounding can be seen in Figures 3.2 and 3.3. Whereas the fence at Tascadero is placed on a slope without being surrounded by big mountains (Fig. 3.4), the end of the fence at Llano is clearly bounded by a high and steep slope (Fig. 3.5). This steep slope has an aspect of ~120°, which is very close to the aspect of ~135° in Tascadero.

Although no precipitation data is available from the weather stations, precipitation generally increases with latitude (Favier et al, 2009). Because Tascadero is located more south, it can be assumed that precipitation is higher there.

Table 3.1: Characteristics at Tascadero and Llano. The average of daily averages are used for temperature and wind speed. For Tascadero values between May 13, 2017 and August 30, 2017 are used. For Llano, values between May 11, 2017 and September 21, 2017 are used.

	Tascadero	Llano
Elevation [m]	3512	3565
Surface inclination [°]	25	0
Aspect [°]	135	0, adjacent slope 120
Average temperature [°C]	-2.7	-2.0
Average wind speed [m/s]	3.5	3.7
Average of daily maximum wind speed [m/s]	6.3	6.5
Prevailing wind direction [°]	0	180
Solar radiation [W/m^2]	176.0	-
Relative humidity [%]	38.2	30.5

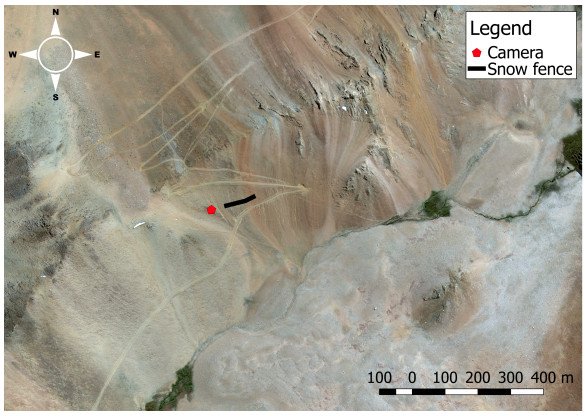

Figure 3.2: Surrounding of Tascadero. A road is located close to the snow fence.

Figure 3.3: Surrounding of Llano. The fence is placed in a valley surrounded by high and steep mountains.

Figure 3.4: Tascadero on May 13, 2017

Figure 3.5: Llano on June 08, 2017

3.2. Snow fences

The wooden snow fences consist of multiples parts (Fig. 3.6) attached to each other using iron pins. Both fences are 2.54 meters high and placed under an angle of 75° with the surface. Their length is different: in Tascadero the fence has a length of 80 meters, whereas the fence in Llano has a length of 33 meters. A photo of a large part of the fence, taken in Llano on October 5, 2017, is shown in Figure 3.7.

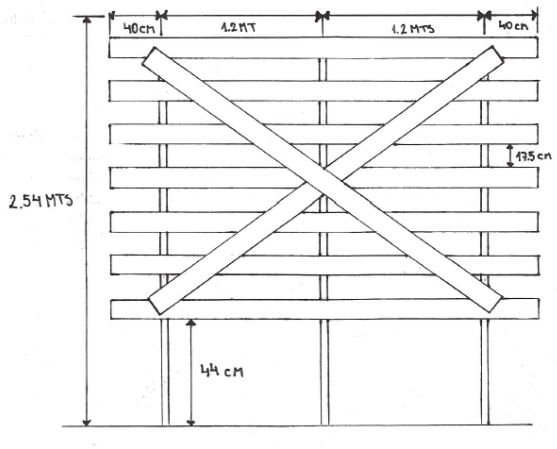

Figure 3.6: Front view and dimensions of one part of the snow fence.

Figure 3.7: Front view of the snow fence in Llano.

3.3. Snow stakes

A grid of bamboo snow stakes were placed adjacent to the snow fence. The stakes around the snow fence were placed such that a large area could be monitored. Schematics of the fences and the grid layouts of the snow stakes for Tascadero and Llano are shown in respectively Figures 3.8 and 3.9. An example of one of the snow stakes is shown in Figure 3.10. Each snow stake is 3 meters tall and has an alternating base color: red-black-red, each covering one meter of the stake. Furthermore, every 10 cm white tape was taped on the stakes.

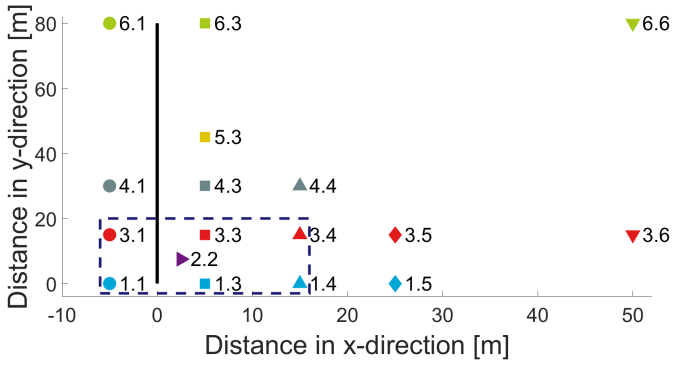

Figure 3.8: Sketch of the snow stakes and fence at Tascadero. The black line represents the fence, the numbered marks indicate the stake locations. The stakes are coloured such that one color represents one line of stakes.

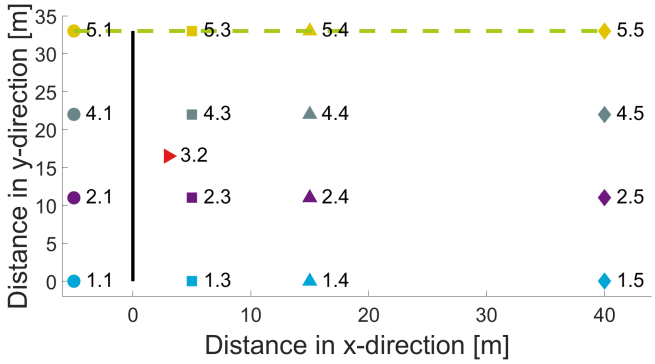

Figure 3.9: Sketch of the snow stakes and fence at Llano. The black line represents the fence, the numbered marks indicate the stake locations. The stakes are coloured such that one color represents one line of stakes.

Figure 3.10: Sketch of the snow stakes and fence at Llano

3.4. Data collection

A digital camera was placed in the extension of the fence. The camera specifications are given in Table 3.2.

Table 3.2: Camera specifications

Brand/type	Canon EOS Rebel T6 / 1300D
Year	2016
Megapixels	18.0
Sensor size	22.3 x 14.9 mm
Pixel dimensions	5184 x 3456
Pixel size	4.3 μ m
Diffraction-Limited Aperature	f/6.9
Aspect ratio	3:2
FOVCF	1.6x
Image processor	DIGIC 4+

The camera was mounted on a mast in a fixed position. However, small differences in camera positioning occurred due to strong winds. Every day photos were taken at 11:00, 12:00 and 13:00. Examples of these photos are shown in Figures 3.4 and 3.5 on page 6. Processing the images to determine the snow depth at each of the stakes is time intensive. Therefore, only one image per week is processed.

On top of the daily camera images, LiDAR measurements were done twice in Tascadero. Once this was done before the first snow fall on March 15, 2017 and once with snow on August 30, 2017 to determine the snow depth and the slope of the surface around the snow fence. Only for stakes *2.2, 1.3, 3.3, 4.3, 5.3, 1.4, 3.4* and *4.4* it was possible to determine the snow depth.

An effort was made to get LiDAR images in Llano as well. However, to obtain useful data, the angle between the LiDAR and surface must be sufficient. This was not the case in Llano and therefore the obtained data did not provide useful information.

Under the assumption that the LiDAR data is very accurate it is useful information for the evaluation of the quality of the different methods.

Furtermore, the exact locations of the snow stakes in Llano were measured using dGPS measurements.

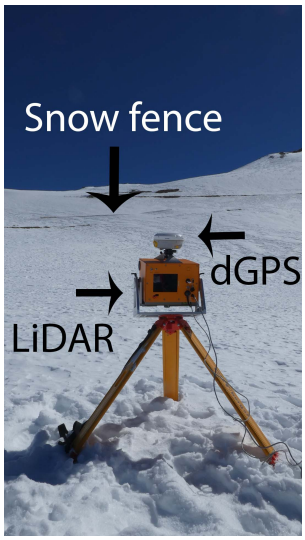

Figure 3.11: Taking LiDAR measurements at Tascadero on August 30, 2017

Figure 3.12: An example of dGPS measurements done in Llano on October 5, 2017. Here, the exact location of the end of the fence is measured. The stakes locations are measured similarly, with the pole of the dGPS device placed on the ground.

3.5. Methods for snow depth calculation

Three distinct methods were used to determine snow depths and are discussed separately in subsections 3.5.1, 3.5.2 and 3.5.3.

3.5.1. Method 1: Manually reading off snow stakes

The first method is based on manually reading off the snow depth at each snow stake, using the white tape markers as a reference. Each stake consists of 30 tapes that are taped on the stakes every 10 cm. Dong and Menzel (2016) used the same method, but they automated the process. Automation was not possible for this research because the snow stakes move substantially due to the influence of wind and snow creep.

Because of the quality of the images, it was not possible to distinguish the tape on all stakes. In Figure 3.8 the dashed blue line marks the area with stakes that were visible enough to calculate snow depths in Tascadero. This area varied for Llano and is therefore not marked in Figure 3.9. In general, the tapes on stakes *4.4, 5.4, 1.5, 2.5, 4.5* and *5.5* were hard to distinguish for Llano. Also, the quality of the images seemed to reduce over time and therefore the usability of this method in Llano is more restricted to time than to area. After August 17, 2017, the quality of the photos was too low to evaluate.

Since the snow stakes bend, their angle deviates from the theoretical 90° angle with the slope. This only occurs when the snow fence is placed on an inclined surface. Therefore it is assumed that the angle in Llano is equal to 90°. This is not the case for Tascadero. From Figure 3.4 it can be seen that the surface has an inclination. The angle between stake and surface is unknown, and has to be estimated using the photos. It is assumed that the stakes only bend in the direction of the slope, perpendicular to the length of the fence. After counting the visible tapes and estimating the angle, equation 3.1 can be used to calculate the snow depth at each snow stake:

$$SnowDepth = (3 - 0.1n) * \sin(\alpha) \tag{3.1}$$

In which n is the number of visible stake parts and α is the estimated angle between the snow stake and the surface. The resulting snow depth is in *meters*.

An example is given in Figure 3.13. The boxes bounded by dashed lines show stakes *1.1, 3.1* and *4.1*. On stake *1.1* the tapes are clearly visible: there are 18 stake parts above the snow surface. Furthermore, the stake has an angle of 90° with the surface. This means that the snow depth at this stake equals $(3-0.1*18)*sin(90) = 1.20$ meter.

The same calculation can be made for stake *3.1*. Although less clear, it is still possible to distinguish the different parts of the stake. For stake *4.1* this is not the case. Therefore, the snow depth at stake *4.1* can not be determined. The snow depth at stake *3.1* equals $(3 - 0.1 * 14.5) * sin(75) = 1.50$ meter.

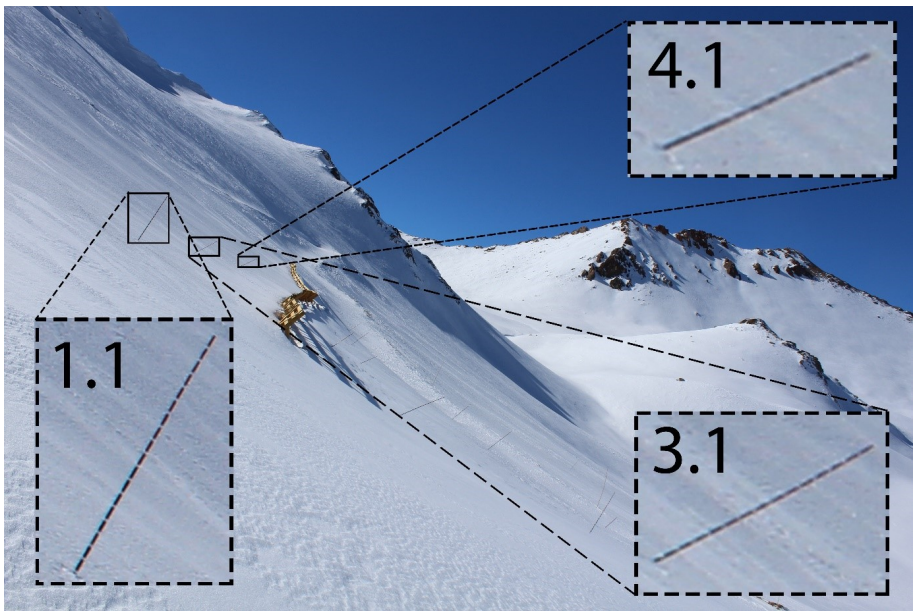

Figure 3.13: Example for method 1 using the photo taken on June 10, 2017. Each stake has a length of 3 meter.

3.5.2. Method 2: Measure the length of the snow stakes

Method 2 is a newly developed method based on the ratio between the measured total length of a stake and the measured length of the visible part of that stake above the snow.

The first step is to georeference the images to an image taken before the first snow fall. This is done in QGIS using *Thin Plate Spine* as transformation type and *Nearest Neighbour* as resampling method because these types gave the most optimal results, e.g. an optimum between deformation of the image and the result of georeferencing was found using these settings. Then, for each stake, and if desired also parts of the fence, the full length is measured in QGIS using the measurement tool. Because the total lengths of the stakes and fence are known to be respectively 3.00 and 2.54 meters, the measured ratio between the full length and visible part can be converted to a snow depth. Similar to method 1, one has to correct for the angle of the stake with the surface. Therefore, the following formula was used:

$$SnowDepth = 3 * (1 - \frac{L_{visible}}{L_{total}}) * \sin(\alpha) \tag{3.2}$$

In this equation, $L_{visible}$ is the length measured in QGIS of the visible part of the stake, e.g. the part of the stake above the snow. This length is measured in arbitrary units. L_{total} must be measured in the same arbitrary units and is the length of the full stake, measured from a photo before the first snowfall occurred. α is the estimated angle between the snow stake and the surface. The unit of the resulting snow depth is *meter*.

Using this method, almost all stakes can be used for evaluation. The restriction depends on the visibility of the snow stakes in the image without snow. Because a white snow background is lacking, the bottom and top of the stakes may be hard to distinguish. Without the (estimate of the) length of the full stake, the snow depth at that specific stake can not be calculated.

An example is given in Figure 3.14, using the photo taken on June 10, 2017. The image with snow is turned because it is georeferenced to the image on the left.

The snow depths for stakes *1.1* and *4.1* are calculated. The lengths (in arbitrary units) of these stakes in the image without snow are respectively 510.188 and 234.443. The visible parts of the stakes in the image with snow have a length of respectively 313.831 and 114.211. The estimated angle between stake *1.1* and the surface is 90°. For stake *4.1* this angle is 75°. The resulting snow depths at these stakes are therefore $3 * (1 - \frac{313.831}{510.188}) * \sin(90) = 1.15$ meter and $3 * (1 - \frac{114.211}{234.443}) * \sin(75) = 1.49$ meter.

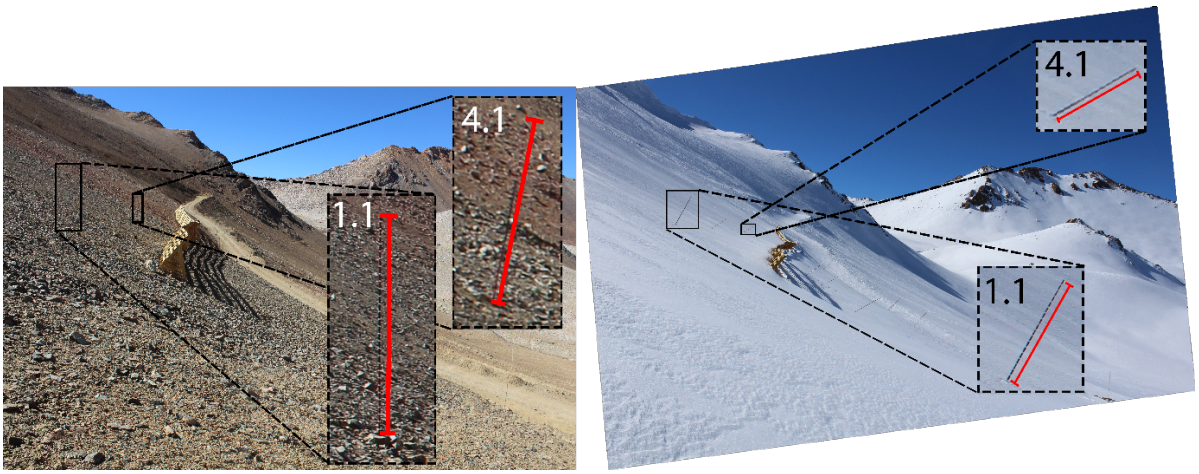

Figure 3.14: Example for method 2 using the photo taken on June 10, 2017. The level of zooming is different and therefore the red lines indicating the length of pnghe stakes do not represent the real length in the image, which is 3.00 meters for both stakes.

3.5.3. Method 3: Combine slope estimation with LiDAR and/or GPS measurements

Method 3 is a new method and is more complicated and more data/tools are needed compared to the first two methods.

In this method, a plane of the snow surface and a plane of the ground surface without snow (Fig. 3.15) are obtained. These are subtracted to calculate the snow depth (Fig. 3.16). The ground surface plane remains fixed in time, while the snow surface plane changes constantly. The necessary steps are listed below.

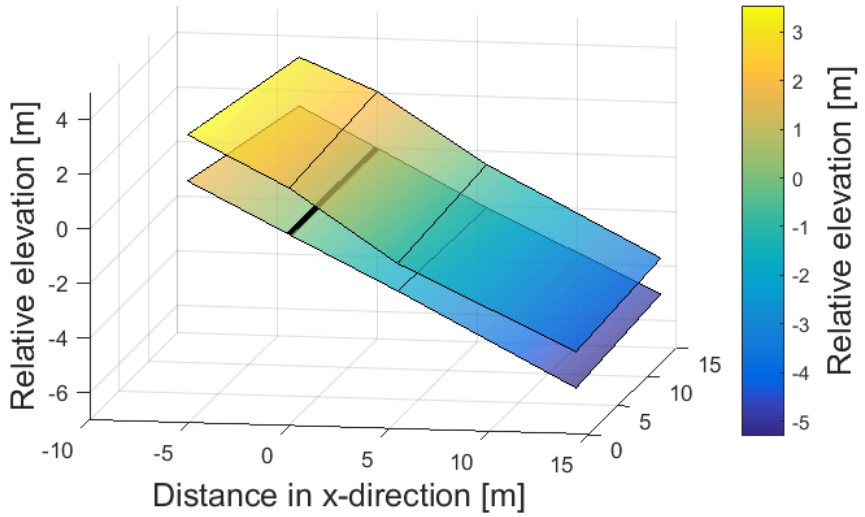

Figure 3.15: A plane of the ground surface without snow and a plane of the snow surface are shown for Tascadero on August 26, 2017. The thick black line marks the bottom of the snow fence.

1. All photos must be georeferenced to the photo without snow because the position of the camera changes slightly over time. This is done in QGIS using *Thin Plate Spline* as transformation type and *Nearest Neighbour* as resampling method.

2. The "true" slope between the snow fence and/or adjacent snow stakes in one row are determined using the dGPS or LiDAR. Row is defined as a line of stakes perpendicular to the fence. An example of one of these rows is marked in Figure 3.9 with the dashed green line. This must be done for the image without snow and the one with snow.

3. Determine the slope in photographs before the winter season (without snow) and on August 30, 2017. This is done in QGIS by drawing triangles and measuring the horizontal and vertical distances between the stakes/fence in one row with the measurement tool in QGIS. Then compute the angle for each part and each situation (with and without snow). An example of this method at Tascadero on August 30, 2017, is shown in Figure 3.17. In this image, only the triangles for the front row are displayed, i.e. stakes *1.1, 1.3* and *1.4*. For Tascadero, there will be 6 triangles in total, 3 for the front row and 3 for the back row. The angle for each part can be computed using the following formula:

$$\alpha = \arctan\left(\frac{L_{vertical}}{L_{horizontal}}\right) \tag{3.3}$$

   In which α is the angle between two points in degrees, $L_{vertical}$ is the vertical length of one triangle in arbitrary units and $L_{horizontal}$ is the horizontal length of the same triangle in the same arbitrary units.

4. Determine the ratio between the slopes computed from the LiDAR/GPS data and the ones from the photos. This must be done individually for each part since the angle under which a part is seen is different and therefore the conversion is different as well. This means that you eventually will have a ratio for the conversion for each line between the stakes in one row. This is important, because the apparent slope measured from the image is different than the considered "real" slope obtained from LiDAR and/or GPS data.

5. In QGIS, measure the height of the full fence in the photo without snow. The height of the fence is known to be 2.54 meter and therefore the ratio between the actual height and the measured height in QGIS, which is an arbitrary number, can be calculated. The value in QGIS depends on the coordinate reference system but will always be arbitrary because the photos are only georeferenced to each other and not to a real location in a specific reference system.

6. Determine the slopes between the stakes and stake/fence for all images processed (e.g. once per week). Use the triangles as shown in Figure 3.17 to accomplish this.

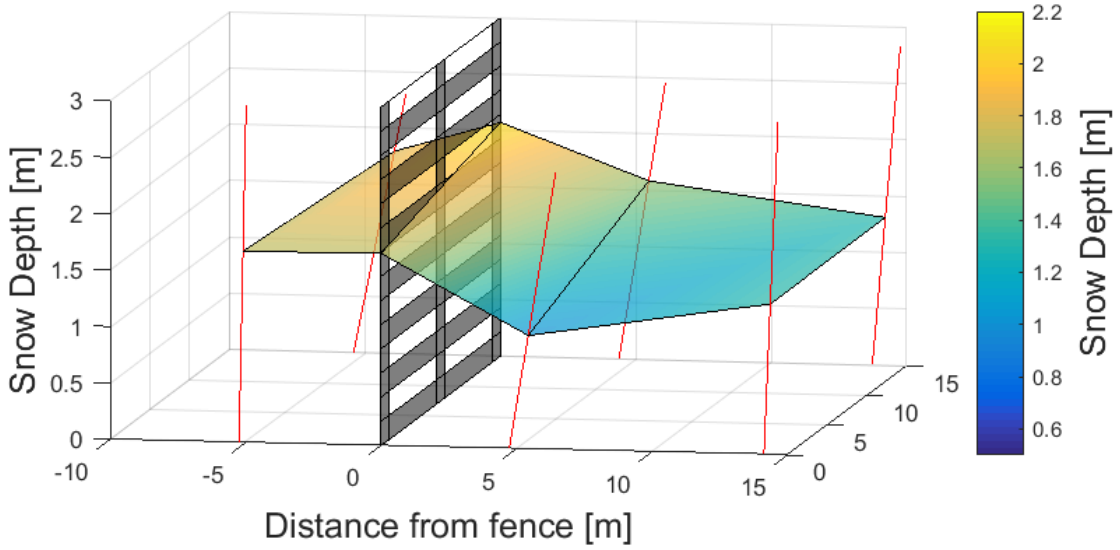

Figure 3.16: Snow depth in Tascadero on August 26, 2017 in 3D representation

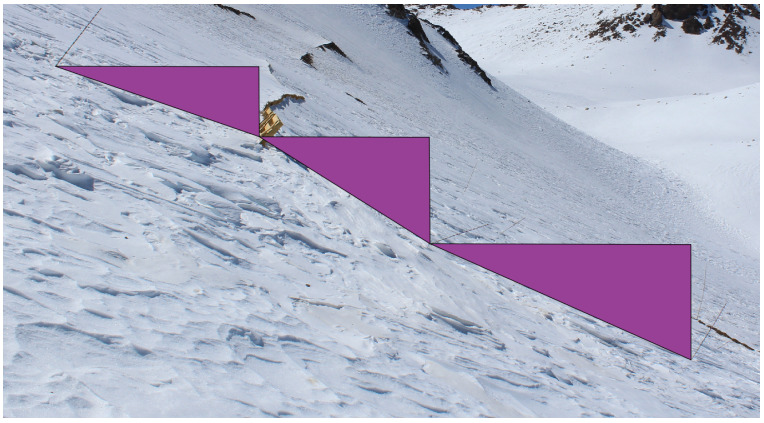

Figure 3.17: Example of the triangles used to calculate the angle between stakes and stakes/fence on August 30, 2017

7. Correct for the obtained angles by multiplying them with the ratio obtained in step 4. The ratio obtained from the photo and LiDAR/dGPS data on August 30, 2017, must be used.

8. Calculate the distance between the stakes/fence from the horizontal and vertical arbitrary distances. This can be done using the Pythagorean theorem:

$$D_i = \sqrt{L^2_{i,vertical} + L^2_{i,ratio}} * D_{ratio,i} \tag{3.4}$$

   In this equation, D_i is the absolute distance in meters between two adjacent measurement points. $D_{ratio,i}$ is the ratio for that distance. This ratio is calculated by dividing the theoretical distance between these stakes/fence and stake by the arbitrary distance value obtained from the photo without snow. So, from the triangles in Figure 3.17 the value for $D_{ratio,i}$ is obtained for each pair of stakes/fence and stake, because the values for D_i are assumed to be known. The values for $D_{ratio,i}$ are then used to calculate D_i for all other photos, where it can be assumed that the stakes have moved and the distances have changed. You do assume in this case that the stakes were placed exactly in one row and that their distances only varies in the x-direction. This assumption can be made since the fence is placed perpendicular to the slope of the hill: stakes will therefore mostly move perpendicular to the fence.

9. Measure the height of the visible part of the fence. Together with the ratio obtained in step 5, the snow depth at the fence can be calculated.

10. Use *Matlab* (or similar software) to create a plane of the hill without snow and the planes of the snow layer for each photo. This is done by using the snow depth at the fence and the angles and distances to the stakes in each line. Note that the movement of the stakes parallel to the fence is not taken into account, they are assumed to only move perpendicular to the fence.

11. Interpolate the plane of the hill to the same distances of the stakes in each plane.

12. Subtract the plane of the hill without snow from each of the planes with snow. The result is the snow depth at each stake and the points at the fence in between. The 3D result is shown in Figure 3.16. A 2D representation is shown in Figure 3.18.

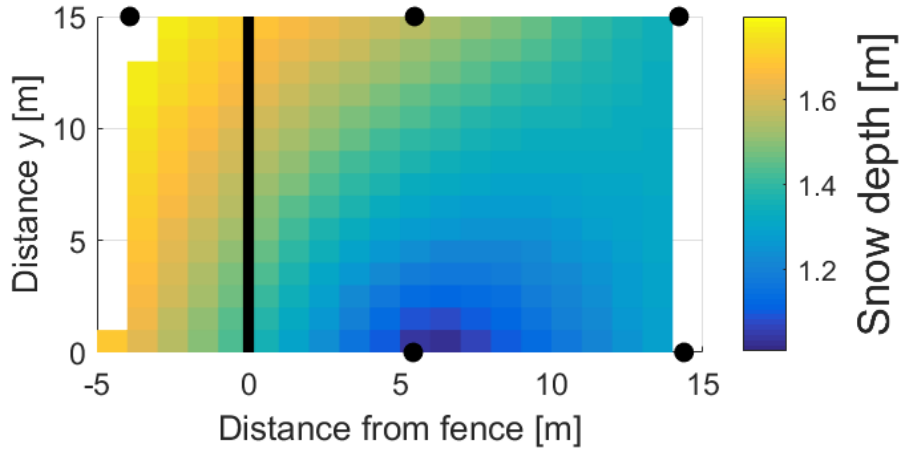

Figure 3.18: Snow depth in Tascadero on August 26, 2017 in 2D representation

3.6. Visualization of snow depths

In chapter 4 the resulting snow depths will be shown in two ways: first as time series plots to illustrate the temporal variability at each snow stake, and secondly as 2D plots to show the spatial variability.

The 2D plots are completed in *Matlab*, using the function *griddata*. This function grids and interpolates irregular data points. This method is required since the stakes (and possibly locations at the fence) are irregularly spaced. For each case, the *'natural'* interpolation method is used.

In order to apply *griddata*, a regular grid must be defined using *meshgrid*. This regular grid is defined once for each method, but the function *griddata* must be applied separately for each moment in time. The following steps are therefore looped to iterate them. Missing data must be flagged so that this data is not used for interpolation. The remaining data is used as an input for *griddata* and the output is the interpolated snow depth at each 1x1 m grid point. The interpolation method *natural* is used as this gave the most realistic results when compared to the photographs. The interpolated data is then visualized using *surf*, which gives a surface plot of the data. Each plot is annotated with the snow fence and location of snow stakes. An example was shown before in Figure 3.18.

3.7. Snow volume calculations

The total snow volume is calculated by summing up the snow depths obtained from the function *griddata*. Because each interpolated value represents the snow depth for 1 m^2, the snow depth values can be summed to find the total volume in cubic meters. To estimate the amount of snow that is present in the area due to the snow fence, an estimate for the snow depth without a snow fence must be made. It is assumed that the stakes further away from the fence are not influenced much by the fence.

Ideally for Tascadero, you would want to take the average snow depth of stakes *1.4, 3.4, 4.4, 1.4, 2.4, 2.5* and *5.3*. This is only possible for method 2 though, because for methods 1 and 3 only the stakes within the area marked with the dashed line in Figure 3.8 are considered. Therefore, the average of stakes *1.3* and *3.3* is assumed to be the snow depth without snow fence for methods 1 and 3.

For Llano the snow depth at all snow stakes is considered, if possible. Therefore, the average of stakes *1.4, 2.4, 4.4, 5.4, 1.5, 2.5, 4.5* and *5.5* is assumed to be the snow depth without a snow fence in place. These stakes are the 8 stakes furthest away from the fence.

To calculate the estimated snow volume without a snow fence, the estimated depth must be multiplied by the area. This area is bounded by the convex hull of the snow stakes. Because the snow stakes that provide data change for both Tascadero and Llano per method/photo, this area changes constantly. Using the matlab function *convexhull*, the area for each method and moment in time can be calculated separately. This area can then be multiplied by the assumed value for the snow depth without a fence.

Subsequently, the estimated snow volume without snow fence must be subtracted from the total volume at that moment in time to find the extra amount of snow that is in place because of the fence.

Because fences at Tascadero and Llano have different dimensions, the results are presented as volume per meter fence, such that results can be compared.

4

Results

In section 4.1 the results of the methods are evaluated. Sections 4.2 and 4.3 present the results of the snow depth and associated volumes for respectively Tascadero and Llano.

4.1. Evaluation of the methods

LiDAR data was obtained for Tascadero on March 15, 2017 and August 30, 2017. Subtracting these data sets gave the snow depth in the area on August 30, 2017 (Fig. 4.1). The result of the interpolated snow depths from the LiDAR data is shown in Figure 4.2.

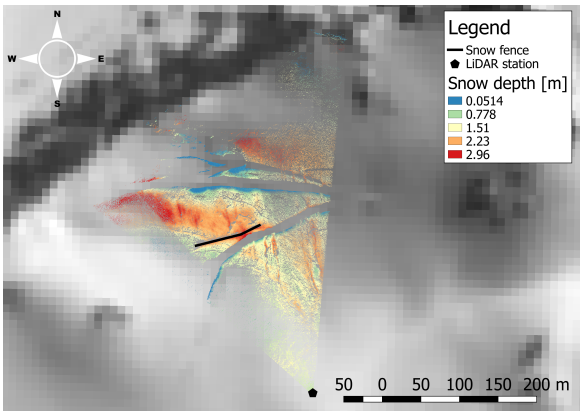

Figure 4.1: The resulting snow depth from two LiDAR datasets on August 30, 2017, covering a Landsat image obtained on September 1, 2017. Because the angle between the LiDAR station and the roads around the snow fence are small the roads are visible because the data is lacking. The LiDAR image was provided by Nicole Schaffer (CEAZA).

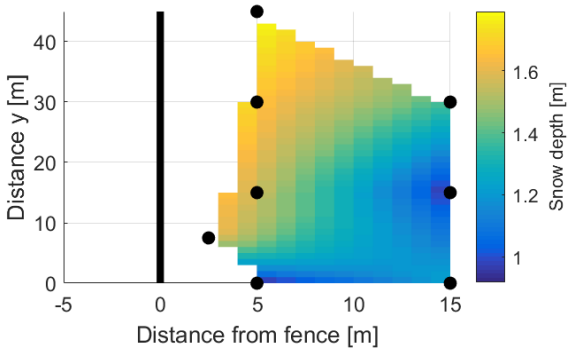

Figure 4.2: Resulting snow depth using the LiDAR data. The values are obtained by calculating the difference between the LiDAR data on March 15, 2017, when no snow was present and on August 30, 2017.

In Table 4.1 the results for the different stakes for which the snow depth could be derived from the LiDAR data on August 30, 2017, are tabulated, together with the available snow stake data from the different methods. Only for method 2 the snow depths at all these stakes were also available. In Table 4.2 the statistics between the snow depths obtained via each of the methods and the LiDAR data are shown. The difference between method 3 and the LiDAR data is larger than the differences between the LiDAR and methods 1 and 2.

In addition to the comparison with the LiDAR data in Tascadero, a comparison between the methods was made for both Tascadero and Llano. For Tascadero, the correlation coefficients between methods 1 and 2 have an average value of 0.97, whereas the average values between methods 1-3 and 2-3 are 0.70 and 0.68 respectively. For Llano the average values were respectively 0.90, 0.67 and 0.53 for methods 1-2, 1-3 and 2-3. The values per stake can be found in Appendix A.

The high similarity to the LiDAR data makes it likely that methods 1 and 2 provide good indications for the snow depths. This suspicion is reinforced by the high correlation coefficients between these methods. Method 2 provides more data than method 1. Therefore the results of method 2 will be presented in this chapter. The results of the other methods are attached in Appendices B and C.

Table 4.1: Snow depths methods compared to LiDAR on August 30, 2017

	LiDAR	Method 1	Method 2	Method 3
Stake 2.2	1.62	1.69	1.62	-
Stake 1.3	0.98	1.02	1.04	1.01
Stake 3.3	1.53	1.53	1.56	1.58
Stake 4.3	1.65	-	1.45	-
Stake 5.3	1.79	-	1.81	-
Stake 1.4	1.23	0.85	0.92	1.33
Stake 3.4	0.92	0.98	0.72	1.30
Stake 4.4	1.38	-	1.10	-

Table 4.2: Statistics of the comparison between snow depths obtained using the different methods and the LiDAR on August 30, 2017. The snow depths obtained via each of the methods is subtracted from the snow depths obtained from the LiDAR.

	Method 1	Method 2	Method 3
Average difference	0.04	0.11	0.51
Standard deviation	0.20	0.15	0.26
Minimum difference	-0.07	-0.06	0.24
Maximum difference	0.39	0.31	0.76

4.2. Snow accumulation Tascadero

The resulting snow depths using method 2 are presented in subsection 4.2.1. The data of the snow depths are used to determine the snow volume around the snow fence. These results are presented in subsection 4.2.2.

4.2.1. Snow depth Tascadero

As can be seen in Figure 3.8 on page 7, the snow stakes in Tascadero were placed such that most of them are close to the camera and snow fence. Therefore, the density of measurement points close to the fence is much higher than further away from the fence.

In Figure 4.3 the snow depth development at each stake over time is shown. The stakes are grouped by column. It can be seen that the time series are correlated.

In Figure 4.4 a part of the photo from May 27, 2017, is provided. The front stake is stake *1.4*, the one furthest away is a stake used to indicate the road. The stake on the right is stake *3.5*. From this image it can be seen that the slope of the hill increases next to the road, and it appears that part of stake *3.5* is not visible because the increased slope blocks the line of view. This has likely resulted in an overestimation of the snow depth at stake *3.5*.

It is also interesting to note that the snow depth at stake *1.1* stays relatively constant, while the snow depth at other stakes in this column increase over time.

In Figure 4.5 the results for all the stakes are shown. The snow depth directly around the fence is higher than the snow depth further away. This difference increases in time. From the photos it is known that the first snow fall occurred just a few days before May 13, 2017. In the first few weeks, the snow is fresh and the influence of the snow fence is limited. It should be noted that stake *1.5* is only visible on the photos of May 13 and 20, 2017. Due to the movement of the camera, the stake was not visible after the 20th of May 2017.

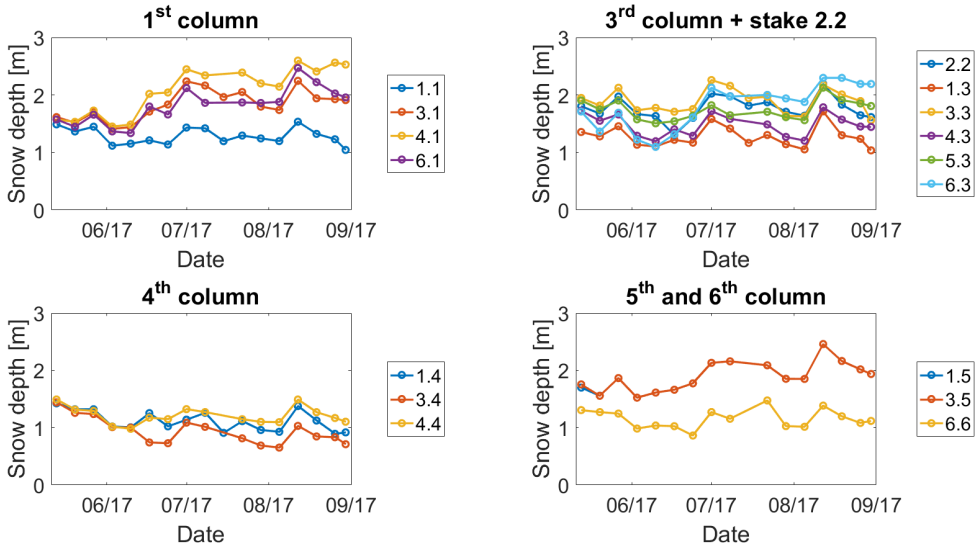

Figure 4.3: Tascadero method 2: Snow depth development per stake in Tascadero between May 13, 2017 and August 30, 2017. Note that stake 1.4 is only measured in the first two photos due to the movement of the camera.

Figure 4.4: Zoomed in photo of stakes 1.3 (foreground) and 2.4 (right). The stake furthest away is a snow stake used to indicate the road.

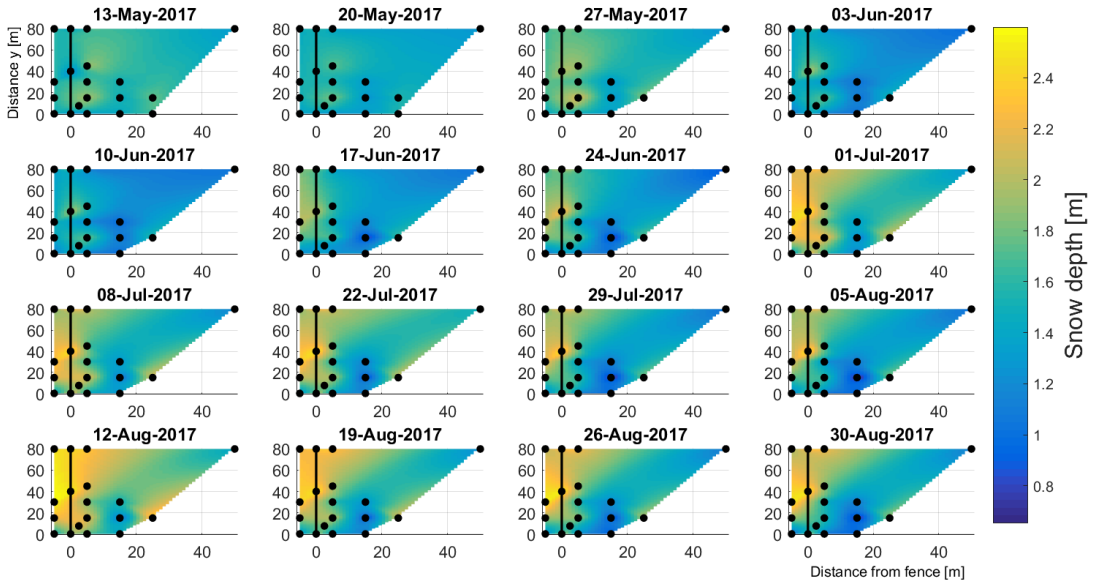

Figure 4.5: Tascadero method 2: Overview of the snow depth development in Tascadero between May 13, 2017 and August 30, 2017.

4.2.2. Volumes Tascadero

Figure 4.6 shows the volume calculations. In this plot it can be seen that the estimated added volume due to the snow fence increases over time, reaching a maximum of ~20 m^3 per meter fence. The percentage of the total volume that is assumed to be in place because of the snow fence initially is about 7% and reaches its maximum of ~30% at the last processed image.

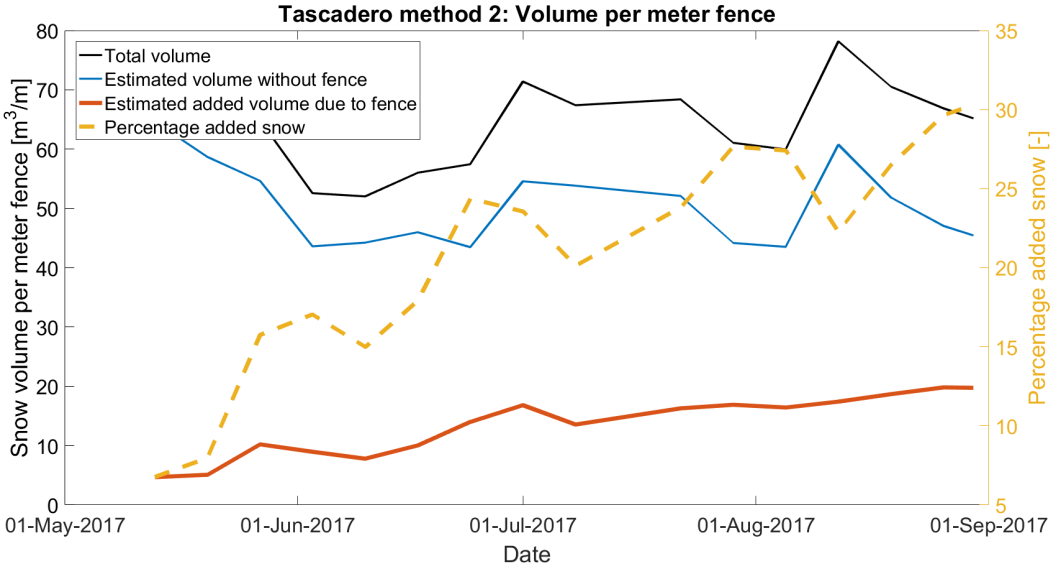

Figure 4.6: Snow volumes calculated for Tascadero using method 2. The total snow volume, estimated snow volume without a fence, added snow volume and percentage of snow due to the presence of a snow fence between May 13, 2017 and August 26, 2017, are plotted.

4.3. Snow accumulation Llano

Similar to the results for Tascadero, the snow depths in Llano are presented first. The second subsection presents the associated volumes in Llano. The results of the snow depths as well as the volumes obtained using methods 1 and 3 are attached in Appendix C.

4.3.1. Snow depth Llano

The snow depth development per stake is shown in Figure 4.7. Photos until September 21, 2017 were evaluated. From the plots of the 4^{th} and 5^{th} column it can be seen that the snow at most of these stakes has already disappeared before the 21^{st} of September 2017.

In the subplot of the 3^{rd} column and stake *3.2* there is a clear jump visible between June and July. This holds for all stakes, except for stake *1.3*. Also, the snow depth at stake *3.2* is slightly lower than the other stakes. In the 5^{th} column the snow depth at stake *4.5* is higher than the other snow depths. This likely is a measurement error, since it can not be seen in the photos. This will be discussed further in chapter 5.

After July, stake *1.5* is not visible anymore due to the movement of the camera.

The 2D representation for Llano is shown in Figure 4.8. Similar to the results per stake in Figure 4.7, it can be seen that around June 22, 2017, the snow depth in column 3 suddenly increases more than the snow depth at other stakes. This is as expected, considering the main wind is coming from the left side of the fence. These results match well with the photos, in which the increased snow depth next to the fence can also be seen. From the photos it can be seen that later in the season, starting around the 24th of August, most of the snow is gone, except for the areas right around the fence and in a lesser extent in column 5. This is also what can be seen in the results. On the last day that was evaluated, September 21, 2017, there is only a little bit of snow left. This small snow patch is located right behind the snow fence: a clear indication that the snow fence does have an effect on the snow volume close to the fence.

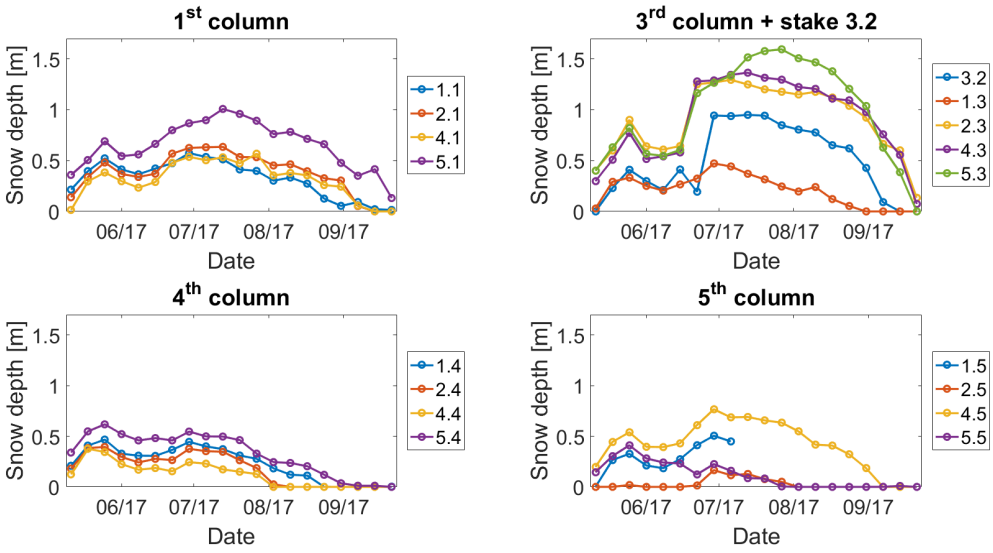

Figure 4.7: Llano method 2: Snow depth development per stake in Llano between May 11, 2017 and September 21, 2017.

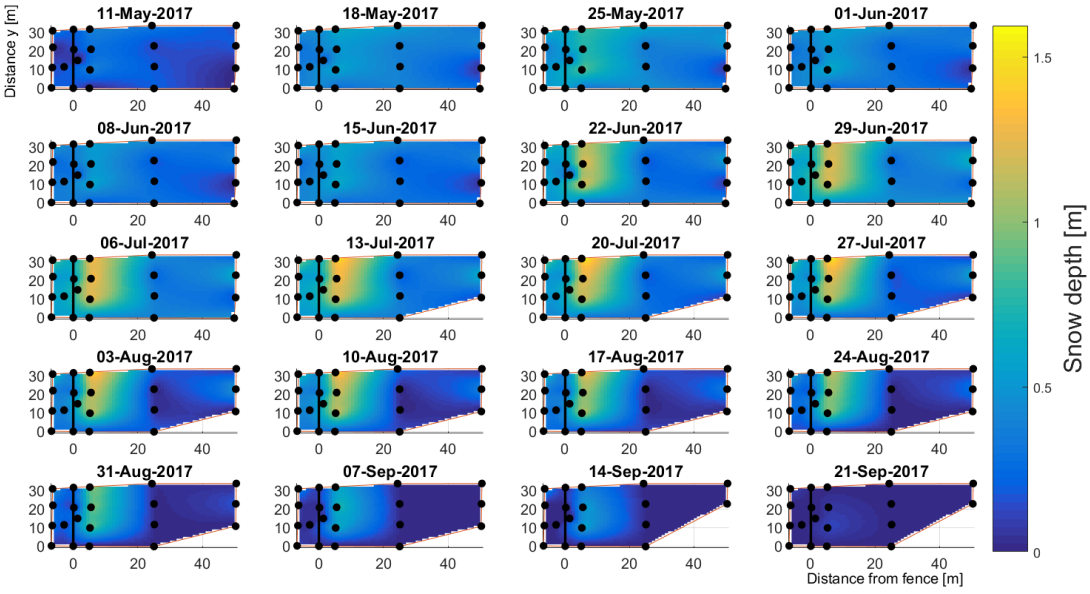

Figure 4.8: Llano method 2: Overview of the snow depth development in Llano between May 11, 2017 and September 21, 2017 The black line represents the snow fence and the black dots show the stakes that were used for the evaluation of that photo.

4.3.2. Volumes Llano

In Figure 4.9 the results of the volume calculations are shown. The maximum added volume due to the fence is ~15 m^3 per meter fence.

The percentage of the total volume that is extra in place due to the snow fence increases a lot. The smallest percentage is ~10%, but reaches almost 100% in September. This corresponds well with the photos, from which we can see that almost all snow has disappeared in September, except for a small snow patch right behind the fence. Assuming this patch is there because of the fence, the percentage should indeed be 100%.

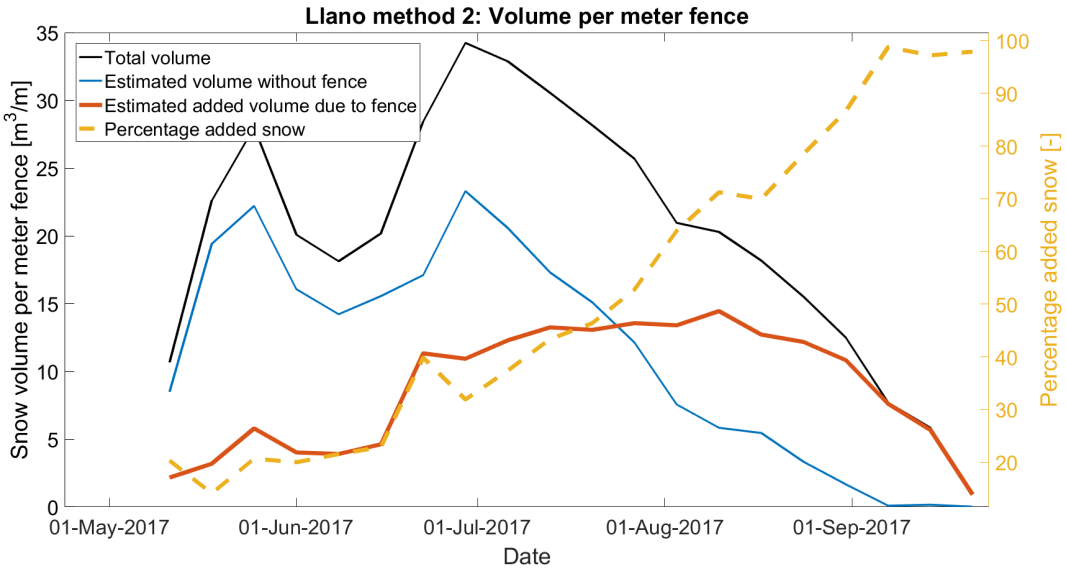

Figure 4.9: Snow volumes calculated for Llano using method 2. The total snow volume, estimated snow volume without a fence, added snow volume and percentage of snow due to the presence of a snow fence between May 11, 2017 and September 21, 2017, are plotted.

5

Discussion & Conclusions

In section 5.1 each of the applied methods will be discussed; what are their advantages and disadvantages? The final subsection of this section discusses what the most optimal method is and why it is recommended for future evaluations. Furthermore, the effectiveness of a snow fence is discussed in section 5.2. In section 5.3 the relevance of this study will be discussed. Finally, recommendations for future research will be given in section 5.4.

5.1. Advantages and disadvantages of the methods

Subsections 5.1.1 to 5.1.3 discuss respectively methods 1 to 3. In the last subsection a conclusion regarding the most optimal method for snow depth determination is presented.

5.1.1. Method 1

Method 1 is an easy way to get fast results, largely because the photos do not need to be georeferenced. Snow depth is determined separately for each snow stake, which prevents errors from propagating. Due to its simplicity, this method was expected to be a reliable method. Wrong assumptions will not significantly change the outcome of the snow depths.

A disadvantage is that the quality of the photos was not high enough to distinguish the tapes on all stakes. Therefore, spatial coverage is poor and restricted to a smaller area close to the camera. Multiple cameras could be installed to overcome this problem. However, this involves additional costs.

Another problem, however only occurring for fences installed on an inclined surface, is that the snow stakes bend. Data can be corrected for this, but the angle between stake and surface must be estimated. It was assumed that the stakes only bend in the direction of the slope, e.g. their position in the y-direction remains the same. Although estimating the angle is subjective and prone to errors, a wrong estimation does not lead to a snow depth that is significantly off. An estimation that is 10° off leads to an overestimated snow depth of maximum 0.37 meter. However, it can be assumed that estimations made are less than 10° off and that the errors are smaller than 0.37 meter. Therefore, the obtained accuracy is high enough for the aim of this project.

On top of this unknown angle, the way the stakes bend is also unknown. It is likely that they bend like 1/4 of an ellipse. Since the eccentricity is hard to estimate, it was assumed that the stakes remain straight.

5.1.2. Method 2

Similar to method 1, method 2 is an easy way to get fast results. However, photos must be georeferenced before measuring the visible part of the stakes. The method can in most cases be applied to all snow stakes and is not restricted to a small area close to the camera.

In contrast to method 1, high quality photos are not required for most images because tapes do not have to be distinguished. Nonetheless, one image of extremely high quality, taken from the same location, is needed to measure the lengths of the full stakes before the first snow fall. Another way could be to paint the stakes such that their contrast with the background colour increases.

For Tascadero, estimates of sufficient quality were made for stakes *5.1, 5.2* and *5.3*. This was not possible for stake *2.5* and this stake was therefore left out of the evaluation. For Llano, estimates were required for

stakes *5.3* and *5.4.* As discussed in section 4.3.1 of chapter 4, snow depths at stake *4.5* were remarkably high; the estimate of the full length was likely to be too small, leading to an overestimation of the snow depth.

Similar to method 1, the angle between the stakes and surface must be estimated. As explained in the previous section, this is not likely to lead to significant errors.

5.1.3. Method 3

Initially, this method was only applied to Tascadero where it showed promising results. However, from comparisons made during a later stage it became clear that the results are likely to be further off from the real snow depth than the other two methods. In particular in Llano some inexplicable large errors occurred at some of the stakes. Therefore the suspicion that this method is not as promising as initially thought grew over time.

Furthermore, it is a time consuming method and additional LiDAR and/or dGPS data is required. Photos also need to be georeferenced.

Similar to method 2, this method requires one high quality photo before the first snow fall. Lower quality images are required for the rest of the season. Because only the place where the stake enters the snow pack has to be measured, dark backgrounds are not a problem for this method.

In contrast to methods 1 and 2, snow depths at the stakes are not determined separately which inserts a risk of error propagation. Errors are summed up which makes snow depths derived at stakes further away from the fence less reliable. This is most probably the reason for the large snow depths in the column of stakes furthest away from the fence in Llano. From a comparison with the photos it is clear that these values can not be correct.

5.1.4. Recommendations on methods for future research

From the correlation coefficients it is clear that the results obtained using methods 1 and 2 are much more correlated to each other than to method 3. A possibility is that these methods cause similar errors and are therefore more correlated. However, the differences between these methods and the snow depths obtained with the LiDAR data also show smaller differences than method 3, as presented in Table 4.2 on page 16. It is therefore likely to assume that methods 1 and 2 provide more reliable results than method 3.

Because method 2 can in most cases be applied to all snow stakes, this method is recommended for future research on snow depth. However, if a very fast idea of the snow depth is required, method 1 could be the best method because images do not have to be georeferenced. Therefore, no additional software except for a photo viewing program is required.

Method 3 would be recommended only for sites where the snow fence is placed on an inclined surface and the background is dark such that the top of the stakes may be hard to distinguish. This could be a location with a very steep slope located directly behind the snow fence. If the slope is too steep to maintain snow it may be hard to see the top of the stakes. In that case, together with the requirement of having an inclined surface, method 3 would be recommended.

5.2. Effectiveness of a snow fence at Tascadero and Llano

Both for Tascadero and Llano the effect of the snow fence is seen in the results. Especially in Llano, where the full cycle from the first snow fall until the moment all the snow has disappeared is captured. Although the snow depths are much lower than in Tascadero, it is clear that at the end of the cycle, between August 31, 2017 and September 21, 2017, all snow in place is there because of the snow fence. This can also be seen in Figures 5.1, 5.2 and 5.3, which show the last 3 photos that were evaluated for Llano: except for the snow located on the hill behind the fence, it is clear that all snow in place is concentrated around the snow fence. Therefore, it can be assumed that this snow patch is there due to the fence.

Figure 5.1: Cropped photo of Llano on September 07, 2017.

Figure 5.2: Cropped photo of Llano on September 14, 2017.

Figure 5.3: Cropped photo of Llano on September 21, 2017.

For Tascadero the fence also has an effect on the snow volume in the area: from Figure 4.6 on page 18 it can be seen that the added snow volume is still increasing at the end of the evaluation period. However, the final effect of the snow fence on the snow depth is unknown because there still is a lot of snow present on August 30, 2017. As the fence does show an effect on snow depth until then, it is expected that the period of snow cover in the area adjacent to the fence will be extended due to the fence.

In Tascadero, the estimated added snow volume reaches a maximum of ~20 m^3 per meter fence, whereas this value is ~15 m^3 per meter fence for Llano. However, the maximum total snow volume in Tascadero (~80 m^3 per meter fence) is much higher than in Llano (~35 m^3 per meter fence). It can therefore also be expected that the absolute effect of the snow fence is higher in Tascadero.

The estimated additional volume is obtained under the assumption that the snow accumulation far away from the fence is not affected by the fence. However, according to the theory as discussed in Chapter 2, the effect of the fence stretches until 30 times the height of the fence. The fence is 2.54 meters high, and should therefore affect snow accumulation up until ~75 meters behind the fence. The stakes that were used to estimate the snow depth without a fence had a distance between 15 and 50 meters from the fence. It is therefore likely that they were affected by the fence. Eventually, this leads to an underestimation of the additional snow volume in place. But, from the snow depth distributions in Tascadero (Fig. 4.5) and Llano (Fig. 4.8), it does not look like the effect of the fence stretches as far as the theory says. However, this is impossible to measure and therefore it can only be concluded that the obtained values for snow volume per meter fence are minimum values.

5.3. Relevance of this study

In this study two new methods (methods 2 and 3) were explored for snow depth derivation from a stake network and camera images. Method 2 proved to provide results very similar to the results of method 1, which had already proved its effectiveness in previous studies. Since the method can be applied to a larger area than method 1 if the same equipment is used, it is promising for future work.

Although it is not applied in this project, it must be possible to semi-automate the process of snow depth derivation using method 2 in a similar way as was done for method 1 by Dong & Menzel (2017).

Previous studies already proved the effectiveness of snow fences, however, this project is the first to examine the effect of snow fences in this region. The influence of the snow fence is clear in both test sites, which is useful information for the regional government.

5.4. Recommendations for future research

For future research it is recommended to further evaluate the possibilities for semi-automating method 2. Whereas only one image per week is used for this project, daily evaluations could be made fast if the process was semi-automated.

In section 5.2 the problem of the unknown distance of the effect of the fence was addressed. This uncer-

tainty could be reduced by doing in situ snow depth measurements during winter in a line perpendicular to the fence. This could help in the understanding of the snow depth distribution behind the fence, such that the distance of the effect of the fence can be determined.

Furthermore it is recommended to further explore the possibilities regarding snow fences in the region. The snow fence at a third site, Guandacol, was completely destroyed. Most probably this happened because of an avalanche. If the regional government decides to place snow fences in the region, more research should be done to find the most optimal locations.

The destruction of the fence at Guandacol also raised the question whether there are any negative side effects of a snow fence. In Guandacol, wood and iron ended up scattered in the area. This can be seen as minor damage to the area, nevertheless it would be interesting to evaluate the environmental impact of such an event. Also, potential negative effects of a snow fence on the surrounding area should be investigated.

It would furthermore be interesting to do more research on the most optimal shape of an snow fence. Modelling the effect of a moon-shaped fence for example could be a first step. Also modelling the effect of multiple fences in a row is interesting. If models do show positive results, these fences could be build on actual test sites to find out which shape and amount of fences is most optimal.

Appendices

A

Correlation coefficients between methods

Table A.1: Correlation coefficients between different methods for Tascadero

Stakes	Methods 1-2	Methods 1-3	Methods 2-3
Stake 1.1	0.96	0.88	0.86
Stake 3.1	0.99	0.60	0.59
Stake 1.3	0.99	0.82	0.80
Stake 3.3	0.99	0.33	0.27
Stake 1.4	0.88	0.92	0.87
Stake 3.4	0.99	0.69	0.67
Average	**0.97**	**0.70**	**0.68**

Table A.2: Correlation coefficients between different methods for Llano. The dashes mean that the correlation coefficient could not be calculated due to too little data points.

Stakes	Methods 1-2	Methods 1-3	Methods 2-3
Stake 1.1	0.79	0.92	1.00
Stake 2.1	0.82	0.70	0.86
Stake 4.1	0.90	0.58	0.70
Stake 5.1	0.94	-0.56	-0.34
Stake 3.2	0.97	0.42	-0.22
Stake 1.3	0.95	0.97	0.90
Stake 2.3	0.99	0.94	0.63
Stake 4.3	0.99	0.95	0.66
Stake 5.3	0.99	0.95	0.36
Stake 1.4	0.76	0.58	0.94
Stake 2.4	0.81	0.61	0.17
Stake 4.4	0.93	-	0.62
Stake 5.4	0.96	-	0.70
Stake 1.5	0.99	1.00	0.99
Stake 2.5	0.73	-	0.14
Stake 4.5	0.97	-	0.82
Stake 5.5	-	-	0.09
Average	**0.90**	**0.67**	**0.53**

B

Results Tascadero methods 1 and 3

B.1. Snow depth development per stake

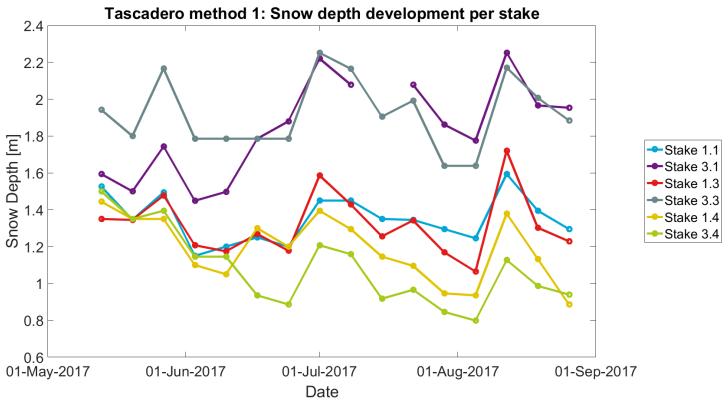

Figure B.1: Tascadero method 1: Snow depth development at each of the stakes between May 13, 2017 and August 26, 2017. Measurement points are indicated using circles.

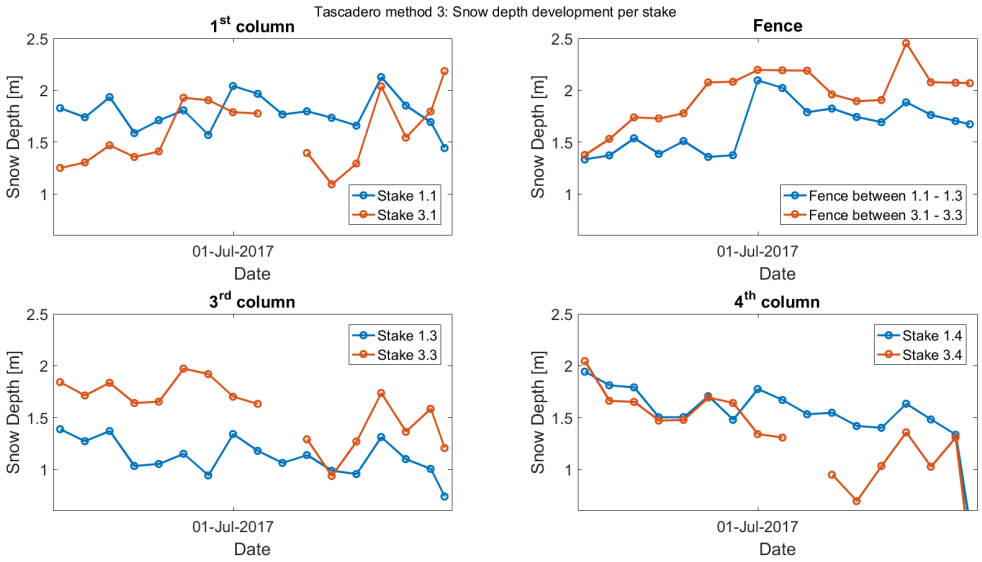

Figure B.2: Tascadero method 3: Snow depth development per stake in Tascadero between May 13, 2017 and August 26, 2017

B.2. 2D representation snow depth

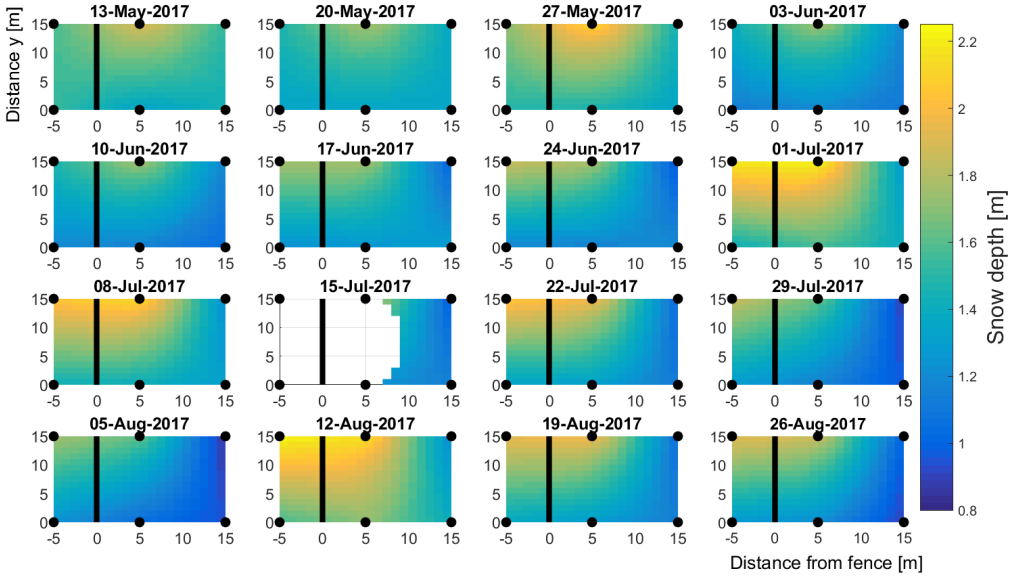

Figure B.3: Tascadero method 1: Snow depth as estimated from the snow stakes between May 13, 2017 and August 26, 2017 at Tascadero. The thick black line represents the snow fence, the black dots show the approximate location of the snow stakes. Although not captured in the Figure, the fence is 80 meters long in reality and does extend further in the y-direction.

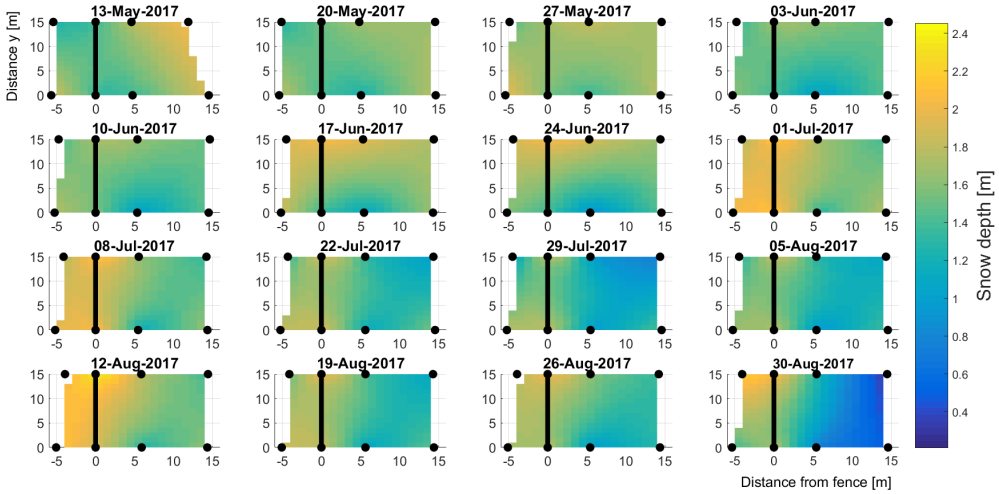

Figure B.4: Tascadero method 3: Overview of the snow depth development in Tascadero between May 13, 2017 and August 30, 2017. The black line represents a sketch of a part of the fence, the black dots indicate the locations of the snow stakes.

B.3. Volume calculations

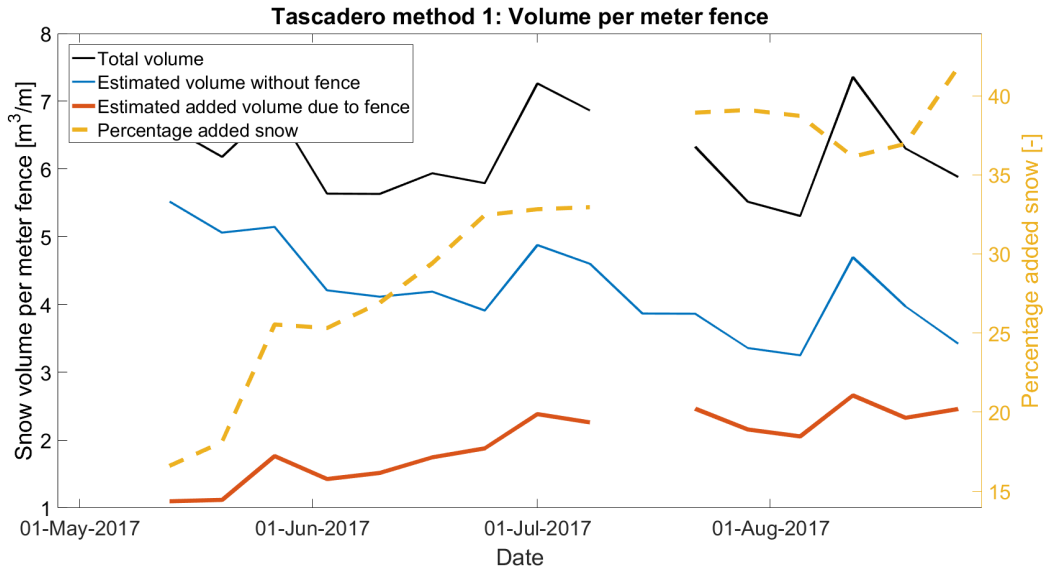

Figure B.5: Snow volumes calculated for Tascadero using method 1. The total snow volume, estimated snow volume without a fence, added snow volume and percentage of snow due to the presence of a snow fence between May 13, 2017 and August 26, 2017, are plotted. The assumed snow depth without snow fence is determined by taking the average of stakes *1.3* and *2.3*.

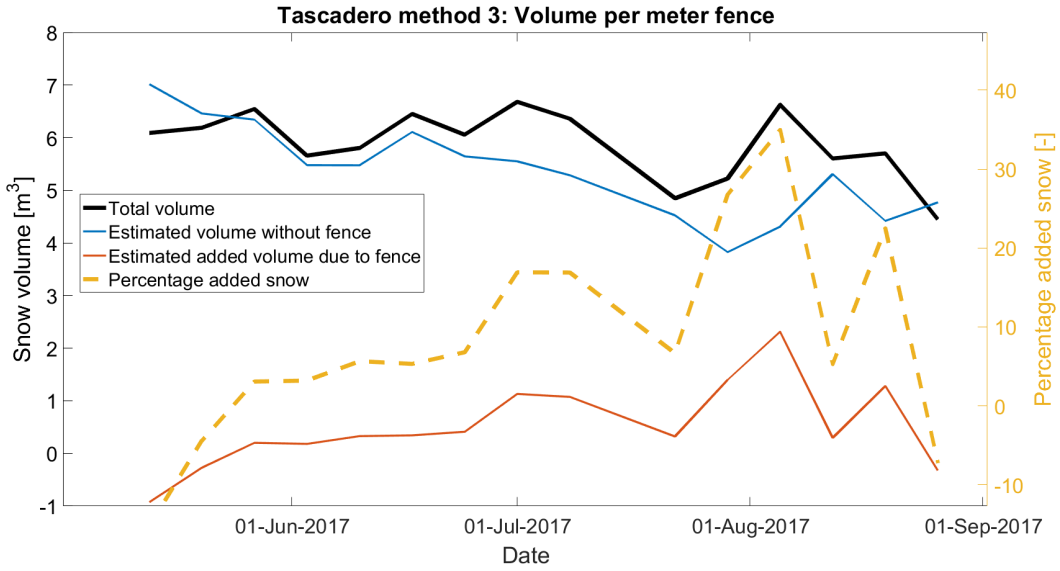

Figure B.6: Snow volumes calculated for Tascadero using method 3. The total snow volume, estimated snow volume without a fence, added snow volume and percentage of snow due to the presence of a snow fence between May 13, 2017 and August 26, 2017, are plotted.

C

Results Llano methods 1 and 3

C.1. Snow depth development per stake

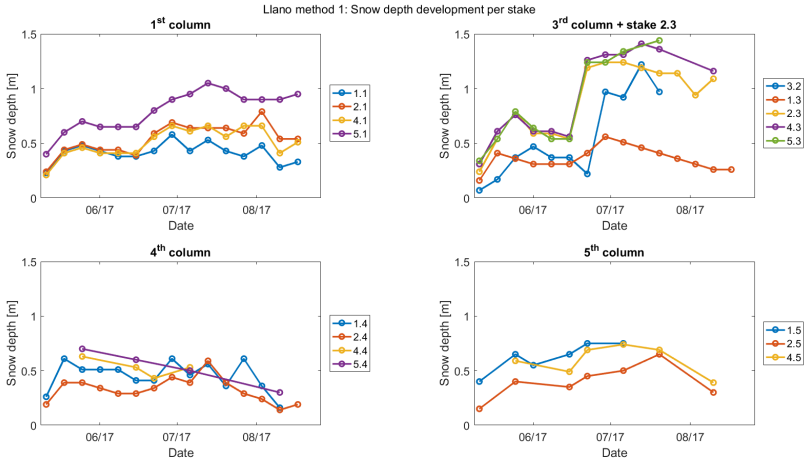

Figure C.1: Llano method 1: Snow depth development at each of the stakes between May 11, 2017 and August 17, 2017 in Llano. Measurement points are indicated using circles. Between these measurement points, values are interpolated.

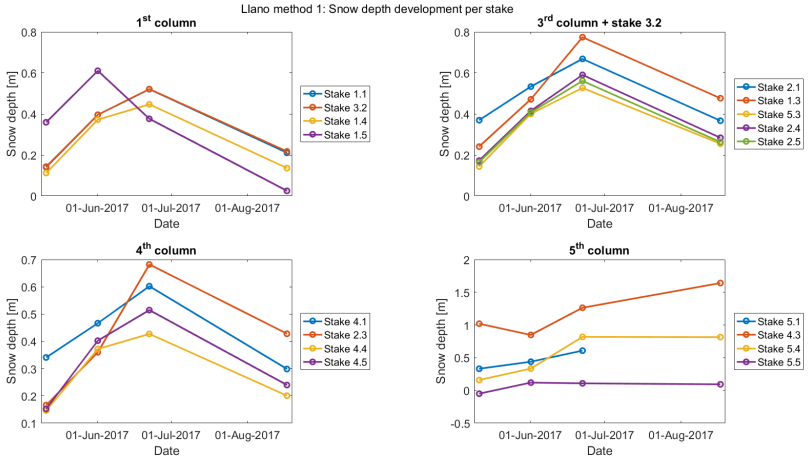

Figure C.2: Llano method 3: Snow depth development per stake in Llano between May 11, 2017, and August 17, 2017. Because only 4 photos were evaluated there are not a lot of data points.

C.2. 2D representation snow depth

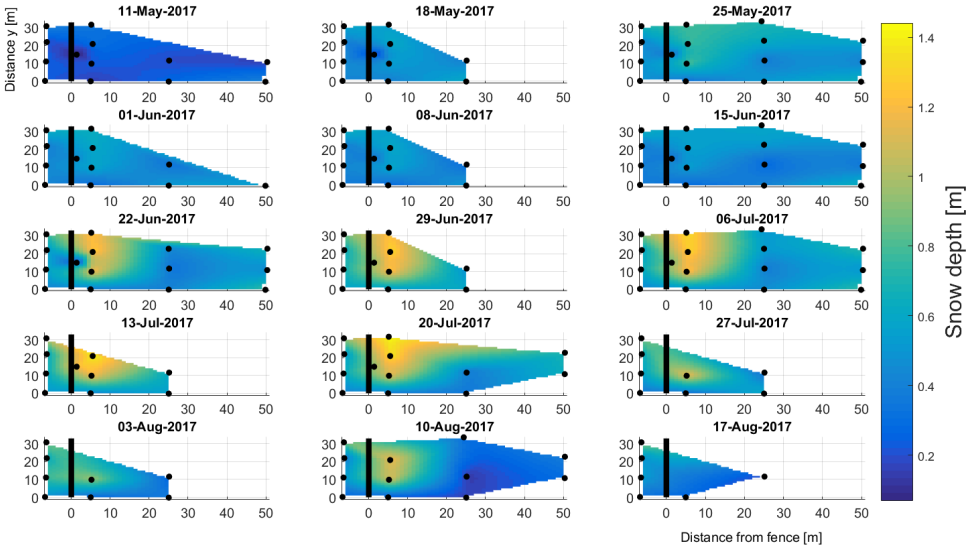

Figure C.3: Llano method 1: Snow depth as estimated from the snow stakes between May 13, 2017 and August 17, 2017 in Llano. Similar to previous plots, the black line represents the fence and the black dots represent the locations of the snow stakes. Only the stakes on which the tapes were countable are plotted. Most of the stakes furthest away from the fence are not visible. After July 20, 2017, the stake closest to the fence, stake 2.1, was no longer visible.

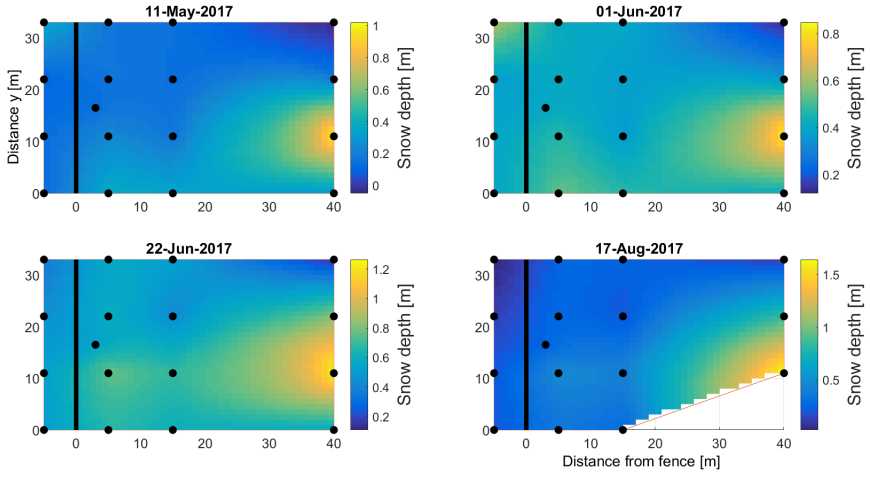

Figure C.4: Llano method 3: Overview of snow depth development in Llano between May 11, 2017 and August 17, 2017. The black line shows the approximate location of the fence, the stakes indicate the locations of the stakes used for evaluation. Note that all stakes could be used, except for stake 5.1 on August 17, 2017. The stake was not visible on the photo at that moment.

C.3. Volume calculations

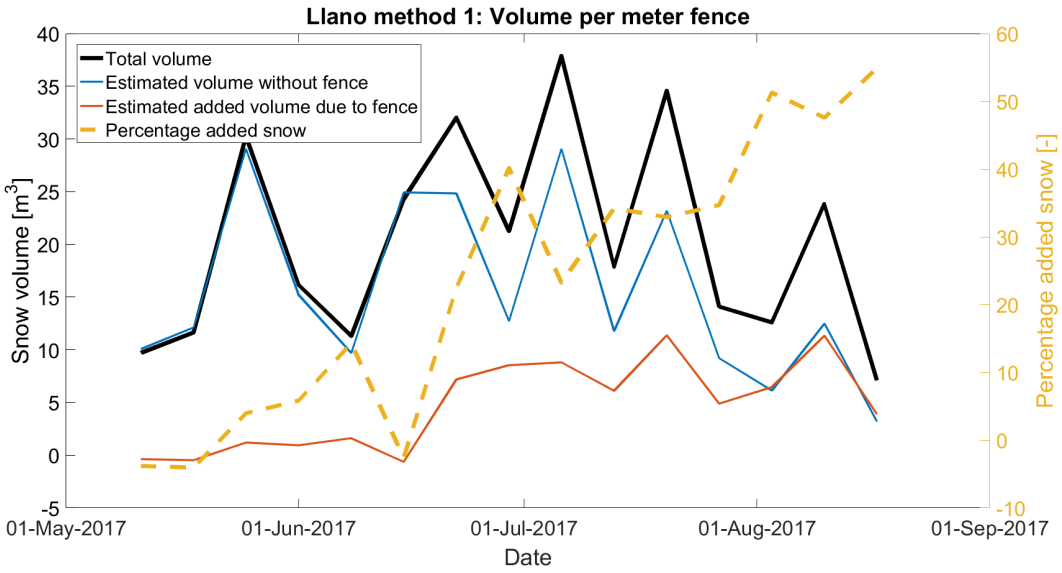

Figure C.5: Snow volumes calculated for Llano using method 1. The total snow volume, estimated snow volume without a fence, added snow volume and percentage of snow due to the presence of a snow fence between May 11, 2017 and August 17, 2017, are plotted.

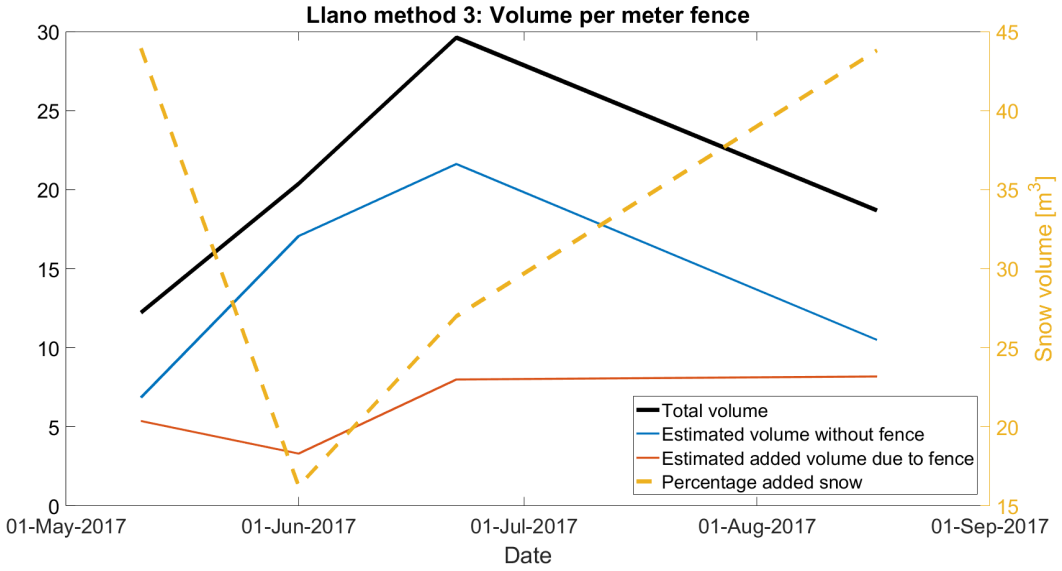

Figure C.6: Snow volumes calculated for Llano using method 3. The total snow volume, estimated snow volume without a fence, added snow volume and percentage of snow due to the presence of a snow fence between May 11, 2017 and August 17, 2017, are plotted.

Bibliography

[1] Patricio Aceituno. On the functioning of the southern oscillation in the south american sector. part i: Surface climate. *Monthly Weather Review*, 116(3):505–524, 1988.

[2] Børre Bang, Anker Nielsen, Per Arne Sundsbø, and Tore Wiik. Computer simulation of wind speed, wind pressure and snow accumulation around buildings (snow-sim). *Energy and buildings*, 21(3):235–243, 1994.

[3] Ruzica Dadic, Rebecca Mott, Michael Lehning, Marco Carenzo, Brian Anderson, and Andrew Mackintosh. Sensitivity of turbulent fluxes to wind speed over snow surfaces in different climatic settings. *Advances in water resources*, 55:178–189, 2013.

[4] Menzel L. Dong C. Snow process monitoring in montane forests with time-lapse photography. *Hydrological Processes*, 2017. doi: https://doi.org/10.1002/hyp.11229.

[5] Fernando Escobar and Patricio Aceituno. Influencia del fenómeno enso sobre la precipitación nival en el sector andino de chile central durante el invierno. *Bulletin de l InstitutFrançaisd'ÈtudesAndines*, 27 (3):753–759, 1998.

[6] Vincent Favier, Mark Falvey, Antoine Rabatel, Estelle Praderio, and David López. Interpreting discrepancies between discharge and precipitation in high-altitude area of chile's norte chico region (26–32° s). *Water Resources Research*, 45(2), 2009.

[7] Koji Fujita, Kuniharu Hiyama, Hajime Iida, and Yutaka Ageta. Self-regulated fluctuations in the ablation of a snow patch over four decades. *Water Resources Research*, 46(11), 2010.

[8] Barichivich J. Boisier J.P. Christie D. Galleguillos M. LeQuesne C. McPhee J. Zambrano-Bigiarini M. Garreaud R., Alvarez-Garreton C. The 2010-2015 mega drought in central chile: Impacts on regional hydroclimate and vegetation. *Hydrology and Earth System Science*, 2017. doi: https://doi.org/10.5194/hess-2017-191w.

[9] Simon Gascoin, Stefaan Lhermitte, Christophe Kinnard, Kirsten Bortels, and Glen E Liston. Wind effects on snow cover in pascua-lama, dry andes of chile. *Advances in Water Resources*, 55:25–39, 2013.

[10] Patrick Ginot, Christoph Kull, Ulrich Schotterer, Margit Schwikowski, and HW Gäggeler. Glacier mass balance reconstruction by sublimation induced enrichment of chemical species on cerro tapado (chilean andes). *Climate of the Past*, 2(1):21–30, 2006.

[11] Jørgen Hinkler, Steen Birkelund Pedersen, Morten Rasch, and Birger Ulf Hansen. Automatic snow cover monitoring at high temporal and spatial resolution, using images taken by a standard digital camera. *International Journal of Remote Sensing*, 23(21):4669–4682, 2002.

[12] Iversen J.D. Comparison of wind-tunnel model and full-scale snow fence drifts. *Journal of Wind Engineering and Industrial Aerodynamics*, 1981. doi: https://drive.google.com/file/d/1GPEBrl89TvIRNayPOuJuhZba8TFL4Y1_/view.

[13] Carlos Le Quesne, David W Stahle, Malcolm K Cleaveland, Matthew D Therrell, Juan Carlos Aravena, and Jonathan Barichivich. Ancient austrocedrus tree-ring chronologies used to reconstruct central chile precipitation variability from ad 1200 to 2000. *Journal of Climate*, 19(22):5731–5744, 2006.

[14] Louis Lliboutry. Glaciers of chile and argentina. *Geological survey professional paper*, 1386(1998):1103, 1998.

[15] R Mott, C Gromke, T Grünewald, and M Lehning. Relative importance of advective heat transport and boundary layer decoupling in the melt dynamics of a patchy snow cover. *Advances in water resources*, 55:88–97, 2013.

[16] Juraj Parajka, Peter Haas, Robert Kirnbauer, Josef Jansa, and Günter Blöschl. Potential of time-lapse photography of snow for hydrological purposes at the small catchment scale. *Hydrological Processes*, 26 (22):3327–3337, 2012.

[17] Tabler R.D. Geometry and density of drifts formed by snow fences. *Journal of Glaciology*, 1980. doi: https://drive.google.com/file/d/1xfzhnEeyx9yFzRCJr90AY9GWgdwYBmQz/view.

[18] Tabler R.D. Snow fence guide. Technical report, Strategic Highway Research Program, 1991.

[19] José Rutllant and Humberto Fuenzalida. Synoptic aspects of the central chile rainfall variability associated with the southern oscillation. *International Journal of Climatology*, 11(1):63–76, 1991.

[20] Alhajraf S. Computational fluid dynamic modelling of drifting particles at porous fences. *Environmental Modelling Software*, 2003. doi: https://drive.google.com/file/d/1f6VdI6bhgxk6q3Dm2merufN0V3mBFjTG/view.

[21] Carla Ximena Salinas, Jorge Gironás, and Miriam Pinto. Water security as a challenge for the sustainability of la serena-coquimbo conurbation in northern chile: global perspectives and adaptation. *Mitigation and Adaptation Strategies for Global Change*, 21(8):1235–1246, 2016.

[22] Baethgen W. Gabriels D. Verbist K., Soto G. Drought mitigation through prediction for an arid zone in chile. *Combating desertification, year=2008*.